Accepted Manuscript

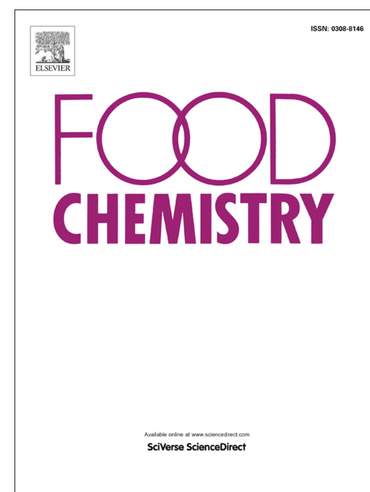

# Characterization and effects of binding of food-derived bioactive phycocyanobilin to bovine serum albumin

Simeon Minic, Dragana Stanic-Vucinic, Mirjana Radomirovic, Milica Radibratovic, Milos Milcic, Milan Nikolic, Tanja Cirkovic Velickovic

PII: S0308-8146(17)31210-4
DOI: http://dx.doi.org/10.1016/j.foodchem.2017.07.066
Reference: FOCH 21450

To appear in: *Food Chemistry*

Received Date: 2 March 2017
Revised Date: 21 June 2017
Accepted Date: 13 July 2017

Please cite this article as: Minic, S., Stanic-Vucinic, D., Radomirovic, M., Radibratovic, M., Milcic, M., Nikolic, M., Cirkovic Velickovic, T., Characterization and effects of binding of food-derived bioactive phycocyanobilin to bovine serum albumin, *Food Chemistry* (2017), doi: http://dx.doi.org/10.1016/j.foodchem.2017.07.066

This is a PDF file of an unedited manuscript that has been accepted for publication. As a service to our customers we are providing this early version of the manuscript. The manuscript will undergo copyediting, typesetting, and review of the resulting proof before it is published in its final form. Please note that during the production process errors may be discovered which could affect the content, and all legal disclaimers that apply to the journal pertain.

1 # Characterization and effects of binding of food-derived bioactive
2 # phycocyanobilin to bovine serum albumin

3 **Simeon Minic [a], Dragana Stanic-Vucinic [a,b], Mirjana Radomirovic [b], Milica**
4 **Radibratovic [c], Milos Milcic [d,e,f], Milan Nikolic [a,b], Tanja Cirkovic Velickovic [a,f,g]***

5 [a]Center of Excellence for Molecular Food Sciences, University of Belgrade - Faculty of
6 Chemistry, Belgrade, Serbia
7 [b] Department of Biochemistry, University of Belgrade - Faculty of Chemistry, Belgrade, Serbia
8 [c] Center for Chemistry - Institute of Chemistry, Technology and Metallurgy, University of
9 Belgrade, Belgrade, Serbia
10 [d] Department of Inorganic Chemistry, University of Belgrade - Faculty of Chemistry, Belgrade,
11 Serbia
12 [e] Center for Computational Chemistry and Bioinformatics, University of Belgrade - Faculty of
13 Chemistry, Belgrade, Serbia
14 [f] Ghent University Global Campus, Yeonsu-gu, Incheon, South Korea
15 [g] Faculty of Bioscience Engineering, Ghent University, Ghent, Belgium
16 *Corresponding author at Ghent University Global Campus, Yeonsu-gu, Incheon, South Korea
17 E-mail address: tanja.velickovic@ghent.ac.kr (TCV)

18 ## Abstract

19 Phycocyanobilin (PCB) is a blue tetrapyrrole chromophore of C-phycocyanin, the main
20 protein of the microalga Spirulina, with numerous proven health-related benefits. We examined
21 binding of PCB to bovine serum albumin (BSA) and how it affects protein and ligand stability.
22 Protein fluorescence quenching and microscale thermophoresis demonstrated high-affinity
23 binding ($K_a = 2 \times 10^6$ $M^{-1}$). Spectroscopic titration with molecular docking analysis revealed two
24 binding sites on BSA, at the inter-domain cleft and at subdomain IB, while CD spectroscopy
25 indicated stereo-selective binding of the *P* conformer of the pigment to the protein. The PCB
26 protein complex showed increased thermal stability. Although complex formation partly masked
27 the antioxidant properties of PCB and BSA, a mutually protective effect against free radical-
28 induced oxidation was found. BSA could be suitable for delivery of PCB as a food colorant or
29 bioactive component. Our results also highlight subtle differences between PCB binding to
30 bovine *vs.* human serum albumin.

31 **Key words:** Spirulina, phycocyanobilin, bovine serum albumin, binding, stability, antioxidant.

32 **Abbreviated (running) title:** Phycocyanobilin binding to BSA.

33 ## 1. Introduction

34 *Arthorspira platensis* or Spirulina, a filamentous cyanobacteria (blue-green microalga),
35 has commonly been used in human and animal nutrition for centuries. Spirulina contains many
36 components of an ideal superfood: a considerable proportion of easily digested complete

37 proteins, carbohydrates, essential fatty acids, pigments, bioavailable vitamins, as well as macro-
38 and micro-elements (**Buono, Langellotti, Martello, Rinna, & Fogliano, 2014**). C-phycocyanin
39 (C-PC), its most abundant single component (14% by dry weight), is a blue biliprotein with
40 proven antioxidant, anti-inflammatory, immune-modulatory, and anti-cancer effects on the
41 human body, primarily due to phycocyanobilin (PCB), a covalently bound linear tetrapyrrole
42 chromophore **(Fernández-Rojas, Hernández-Juárez, & Pedraza-Chaverri, 2014**). Both C-PC
43 and PCB show great potential for applications in biotechnology, medicine, and the food industry
44 (as food colorants) **(Eriksen, 2008; McCarty, 2007**).

45 Bovine serum albumin (BSA) is the major protein of bovine blood plasma, as well as a
46 dietary protein found in beef and cow's milk **(Fuentes Aparicio, Sanchez Marcen, Perez**
47 **Montero, Baeza, & de Barrio Fernandez, 2005**). BSA is an α-helicoidal globular protein
48 composed of a single polypeptide chain with 583 amino acid residues, organized into three
49 homologous domains (I, II, and III), each of which contains two subdomains, termed A and B
50 (**Bujacz, 2012; Peters, 1995**). It is one of the most extensively studied proteins and has
51 applications in various life science disciplines and as a model system for studying protein-ligand
52 interactions. Due to its emulsifying properties, BSA is used as a food additive **(Ofori & Hsieh,**
53 **2012**). BSA is also a versatile carrier for various drugs and nutraceuticals (**Livney, 2010**).

54 Bilirubin and biliverdin, bioactive PCB tetrapyrrole analogs found in animals, have a high
55 propensity to interact with serum albumins (**Peters, 1995**). Our research group recently
56 demonstrated that PCB binds with high affinity to human serum albumin (HSA) (**Minic, Milcic,**
57 **Stanic-Vucinic, Radibratovic, Sotiroudis, Nikolic, et al., 2015**), increasing protein thermal and

58 proteolytic stability (**Radibratovic, Minic, Stanic-Vucinic, Nikolic, Milcic, & Velickovic,**
59 **2016**). Bioactive ligand binding may affect the flexibility and stability of a food protein,
60 changing its folding and digestion (**Celej, Montich, & Fidelio, 2003; Stojadinovic,**
61 **Radosavljevic, Ognjenovic, Vesic, Prodic, Stanic-Vucinic, et al., 2013**), as well as ligand
62 bioavailability and bioactive properties, such as antioxidant activity (**Jakobek, 2015**). Therefore,
63 examination of the interactions between food-derived proteins and bioactive molecules can yield
64 valuable information about their distribution, stability, and activities *in vivo*.

65 Due to its low cost and acceptance in the food and pharmaceutical sector, BSA is widely
66 used as delivery vehicle for drugs and bioactive compounds (e.g. polyphenols), based on its
67 noncovalent interactions with low molecular mass molecules. There are only few studies dealing
68 with interactions of PCB with proteins, reporting binding to HSA (**Minic, et al., 2015;**
69 **Radibratovic, et al., 2016**). Numerous studies demonstrated that interactions with proteins can
70 protect redox sensitive bioactive nutriceuticals, but literature data on effects of PCB-protein
71 interactions on the PCB stability and antioxidative activity of the PCB-protein complex are still
72 missing. Therefore, in this study we characterized for the first time the binding of PCB to BSA,
73 compared our findings with those from the HSA-PCB complex, and then examined the effects of
74 binding on the thermal and oxidative stability of both protein and ligand. Binding parameters,
75 established by fluorescence quenching, spectrophotometric titration, and microscale
76 thermophoresis (MST) experiments, revealed high-affinity PCB binding to BSA. CD
77 spectroscopy indicated stereo-selective *P*-conformer ligand binding. Molecular docking analysis
78 identified two specific ligand binding sites on the protein, different from those on HSA, as well

79 as a potential interaction pattern. The consequences of binding were analyzed by far-UV CD
80 spectroscopy, in antioxidant assays, and by monitoring of free radical-induced oxidation.
81 Increased stability of both interacting partners suggest that BSA can serve as suitable delivery
82 system for bioactive PCB.

## 83 2. Materials and methods

### 84 *2.1. Materials*

85 Essentially globulin free BSA (≥99%) was purchased from Sigma-Aldrich (USA) and
86 used without further purification. BSA concentration was determined spectrophotometrically
87 using the extinction coefficient of 43 824 $M^{-1}cm^{-1}$ at 279 nm. PCB was purified from commercial
88 Hawaiian *Spirulina pacifica* powder (Nutrex, USA) and then quantified from stock solutions in
89 DMSO as previously described (**Minic, Milcic, Stanic-Vucinic, Radibratovic, Sotiroudis,**
90 **Nikolic, et al., 2015**). All experiments (except for antioxidant assays, see below) were done in 20
91 mM Tris buffer, pH 7.2. Final concentrations of DMSO in BSA-PCB mixtures did not exceed
92 1% (v/v). Reagents for MST measurements were generous gift from NanoTemper, Germany. All
93 other chemicals were of analytical reagent grade and Milli-Q water (Millipore, France) was used
94 as a solvent.

### 95 *2.2. Fluorescence quenching measurements*

96 The fluorescence spectra were recorded with a FluoroMax®-4 spectrofluorometer
97 (HORIBA Scientific, Japan). Experimental details and fluorescence quenching analysis are given
98 in Supplementary data (Appendix A).

99 *2.3. Microscale thermophoresis measurements*

100 Lysine residues in BSA were covalently labeled with fluorescent dye NT-547 using the
101 Monolith™ NT.115 Protein Labeling Kit GREEN-NHS (NanoTemper Technologies GmhH,
102 Germany) according to the supplied labeling protocol. PCB was serially diluted over five orders
103 of magnitude (between 200 μM and 6 nM) in MST buffer containing 0.05% Tween-20. Labeled
104 BSA was mixed 1:1 (vol/vol) with pigment dilutions. The final concentration of labeled protein
105 in BSA-PCB mixtures was 1.5 μM. The samples were loaded into the Monolith™ NT.115
106 premium coated capillaries (NanoTemper Technologies), and incubated at ambient temperature
107 for 30 min. Capillaries were then placed in the Monolith NT.115 instrument (NanoTemper
108 Technologies). Typically, LED and MST power were set to 20 and 40%, respectively, and green
109 LED-filter was used. Obtained data were plotted as the relative fluorescence versus the logarithm
110 of PCB concentrations. The dissociation constant ($K_d$) was estimated using the NanoTemper
111 analysis software version 1.5.41 (NanoTemper Technologies).

112 *2.4. UV/VIS absorbance measurements*

113 UV/VIS absorption spectra were recorded on a NanoDrop 2000c spectrophotometer
114 (Thermo Scientific, USA) in a quartz cuvette with 1.0 cm path length. The measurements of 20
115 μM PCB in the absence and presence of BSA (10, 20 and 40 μM) were made in the range of
116 300-750 nm at room temperature. Stoichiometry determination of PCB binding to BSA was
117 determined by titration of 20 μM PCB solution with 1 mM BSA stock solution in order to obtain
118 the BSA/PCB molar ratios between 0 and 1.5. After absorbance measurements, plot of
119 absorbance dependence at 365 nm on BSA/PCB molar ratio was constructed. The reciprocal

120 value of intersection point between the linear part of the curve and plateau phase gives the
121 number of ligand moles bound per mole of protein.

122 *2.5. CD spectroscopy measurements*

123 All CD measurements were carried out on Jasco J-815 spectropolarimeter (Jasco, Japan)
124 under thermostated conditions. For the measurements in the near-UV and visible region (250-
125 700 nm), concentration of BSA was 10 μM, while concentrations of PCB varied from 0 to 30
126 μM. All spectra in the near-UV and visible region were recorded at 25$^{o}$C. BSA thermal
127 denaturation experiment was performed at the temperature range 37-93$^{o}$C, with temperature
128 increasing rate 2°C/min. Equilibration time for each temperature was set to 1 min. Ellipticity was
129 measured in far-UV region at 222 nm with pathlength cells of 1 cm. Concentration of BSA was
130 0.5 μM, while PCB concentrations were 0.5 and 1 μM. Results were expressed as dependence of
131 percentage of the initial ellipticity (at 37$^{o}$C), taken as 100%, on temperature. Obtained plots were
132 fitted with a sigmoidal function. The inflection point in the plot was taken as melting temperature
133 ($T_m$) of BSA.

134 *2.6. Molecular docking*

135 The crystal structure of the BSA was downloaded from the Protein Data Bank (PDB ID:
136 3v03) and the AutoDockVina program (**Trott & Olson, 2010**) was used for performing
137 molecular docking study on BSA-PCB complex. The details of the docking study are presented
138 in Supplementary data (Appendix A).

139 *2.7. BSA and PCB oxidation by free radicals*

140 BSA oxidation induced by free radicals, obtained by the decomposition of 2,2'-azobis(2-
141 amidinopropane) dihydrochloride (AAPH), was monitored using protein intrinsic fluorescence as
142 a probe. BSA solutions (1 μM) in the absence (blank) and presence of PCB (1 and 2 μM) or
143 standard antioxidant Trolox (2 μM) were pre-incubated at 37$^{o}$C during 15 min. Reaction was
144 initiated by addition of AAPH stock solution (500 mM) to obtain 25 mM final concentration
145 mixture. Excitation and emission wavelengths were of 280 and 340 nm, respectively, and slits
146 were set to 5 nm. Fluorescence decay was recorded during 30 min. Fluorescence contribution of
147 PCB was subtracted. Protective effect (PE) of PCB against BSA oxidation was quantified in
148 arbitrary units (a.u.) using equation:

149 $$PE(a.u) = AUC_{BSA+PCB} - AUC_{freeBSA} (1)$$

150 Where PE represents PCB protective effect, while AUC represents area under curve for
151 respective samples.

152 PCB oxidation, induced by free radicals obtained by the decomposition of AAPH, was
153 monitored using pigment absorbance as a probe. PCB solutions (50 μM) in the absence (blank)
154 and presence of BSA (25, 50 and 250 μM) were pre-incubated at 37$^{o}$C during 5 min. Reaction
155 was initiated by addition of AAPH stock solution (500 mM) to obtain 28 mM final concentration
156 mixture. Reaction mixtures were incubated at 37$^{o}$C. UV/VIS absorption spectra were recorded in
157 the range of 300-750 nm at 0 (samples without AAPH), 10 and 30 min after initiation of
158 reaction. In order to monitor absorbance changes at 620 and 560 nm during time, samples with
159 the same concentrations of BSA, PCB and AAPH were prepared as previously described.
160 Absorbances were recorded during 30 min at 37$^{o}$C.

161 *2.8. Antioxidant assays*

162 Oxygen radical absorbance capacity (ORAC) assay was performed as described **(Ou,**
163 **Hampsch-Woodill, & Prior, 2001**) with some modifications **(Minic, Stanic-Vucinic,**
164 **Mihailovic, Krstic, Nikolic, & Velickovic, 2016**). Briefly, stock solutions of fluorescein (5
165 μM), free radical generator AAPH (500 mM) and various samples were made in 75 mM
166 potassium phosphate buffer, pH 7.4. 250 μL of sample solutions (BSA, PCB and BSA-PCB
167 complexes) or Trolox were mixed with 1485 μL and 15 μL of buffer and fluorescein solution,
168 respectively. The reaction was initiated by adding 250 μL of AAPH solution. Excitation and
169 emission wavelengths were 485 and 511 nm, respectively, and slits were set to 2 nm. The
170 relative sample ORAC value was expressed as Trolox equivalents (TE).

171 The reducing power of BSA, PCB and BSA-PCB complex samples was measured
172 according to modified original method (**Oyaizu, 1986**). 40 μL of sample solution was added to
173 100 μL of 0.2 M phosphate buffer, pH 6.6 and 100 μL of 1% potassium hexacyanoferrate(III).
174 After incubation at 50°C during 20 min, 50 μL of 20% trichloroacetic acid was added to the
175 reaction mixture, followed by centrifugation at 10000xg during 15 min. A 100 μL of supernatant
176 was mixed with 100 μL of Milli-Q water and 12 μL of 0.1% $FeCl_3$. After 10 min incubation on
177 room temperature absorbance was measured at 670 nm.

178 For both assays, masking effect (ME) of the PCB antioxidant capacity was calculated
179 using equation:

180 $$\mathbf{ME}\,(\%) = \mathbf{100}\% - \left(\mathbf{100} * \frac{\mathbf{AC_{BSA-PCB}}}{\mathbf{AC_{BSA}+AC_{PCB}}}\right)\%\ (\mathbf{2})$$

181 Where, $AC_{BSA\text{-}PCB}$, $AC_{BSA}$ and $AC_{PCB}$ represent antioxidant capacities of BSA-PCB

182 complexes, free BSA and free PCB, respectively.

## 183 3. Results

### 184 *3.1. Detection and characterization of PCB binding to BSA*

#### 185 *3.1.1. PCB quenches BSA intrinsic fluorescence*

186 Ligand binding often induces quenching of protein intrinsic fluorescence. The presence of
187 two tryptophan residues in BSA produces strong protein emission upon excitation at 280 nm.
188 Addition of PCB in gradually increasing concentrations induced a significant decrease in BSA
189 fluorescence, followed with a blue shift of the emission maximum, from 342 to 335 nm (**Fig.
190 1A**). **Fig. 1B** shows the Stern-Volmer (SV) plot for quenching of BSA fluorescence by PCB. The
191 slope of this curve indicates an SV quenching constant of $1.7 \times 10^{6}$ $M^{-1}$, with a bimolecular
192 quenching rate constant of $1.7 \times 10^{14}$ $M^{-1}s^{-1}$, which is four orders of magnitude higher than the
193 diffusion rates of biomolecules ($10^{10}$ $M^{-1}s^{-1}$). These data suggest that static (contact) quenching
194 of BSA fluorescence by PCB occurs. The calculated binding constant of $2.3 \times 10^{6}$ $M^{-1}$ at 25°C
195 (**Fig. S1**) indicates high-affinity binding site(s) for PCB on BSA.

196 Synchronous fluorescence is a useful approach to separate the contribution of Trp and
197 Tyr residues to total protein intrinsic fluorescence. From **Figs. 1C and 1D**, it is clear that the
198 binding of PCB induced greater Trp residues fluorescence quenching, in comparison to the
199 decrease in fluorescence arising from Tyr residues, with no significant shifts of emission
200 maxima, indicating that bound PCB was situated closer to Trp residues. Therefore, the blue shift
201 seen in basic BSA fluorescence spectra (**Fig. 1A**) is due to preferential quenching of the Trp
202 residues by PCB binding, while the relative contribution of Tyr residues to protein fluorescence

203 increases upon ligand binding.

204 *3.1.2. PCB changes the thermophoretic mobility of BSA*

205 MST is a relatively new method for characterization of ligand-macromolecule binding. It
206 is a fluorescence-based technique, in which an infrared laser generates a microscopic
207 temperature gradient in sample capillaries. Protein mobility across a temperature gradient differs
208 following ligand binding due to changes in its surface area, effective charge, and hydration
209 entropy **(Wienken, Baaske, Rothbauer, Braun, & Duhr, 2010**). As can be seen from **Fig. 2A**,
210 fluorescently labeled BSA moves from a locally heated region to the outer cold region until a
211 steady-state is reached (up to 30 s). Addition of PCB decreased protein thermophoretic mobility
212 and consequently increased the normalized fluorescence. A $K_d$ value of 0.738 μM was calculated
213 from the obtained binding curve (**Fig. 2B**), whereas the binding constant is $1.4 \times 10^6$ $M^{-1}$
214 ($K_a$=1/$K_d$), a value comparable to that obtained from the fluorescence experiments.

215 *3.1.3. Addition of BSA changes absorption and CD spectra of PCB*

216 The binding of PCB to proteins was monitored based on changes in chromophore
217 UV/VIS spectra. Remarkably, addition of BSA to the PCB solution induced an instant color
218 change, visible to the naked eye, from blue to green, indicating complex formation (**Fig. 3A**).
219 Absorption spectra confirmed the BSA-induced red shift in the near-UV and VIS spectra of
220 PCB, from 365 to 369 nm and from 602 to 606 nm, respectively (**Fig. 3B**). It was also observed
221 that BSA decreased PCB absorbance across the entire range of the measured values, with the
222 exception of the appearance of a peak ("shoulder") at 405 nm. As yellow chromophores absorb at
223 405 nm, the appearance of this peak shoulder, together with the contribution of the red shift of

224 the peak at 602 nm, is responsible for shifting the blue color toward the green observed in the
225 PCB-BSA complex. The ability of BSA to significantly decrease the absorbance of PCB at 365
226 nm was used to determine the stoichiometry of the BSA-PCB binding complex. The two-phase
227 profile was obtained after spectrophotometric titration of PCB with BSA (**Fig. 3C**). At lower
228 BSA/PCB ratios, the decrease in pigment absorbance was linear, while at higher BSA
229 concentrations a plateau was obtained. Intersection between these two phases at a BSA/PCB
230 ratio of 0.553 yielded 1.81 moles of PCB per mole of BSA, indicating a binding stoichiometry of
231 2:1 (two moles of PCB per mole of BSA).

232 In aqueous solutions, free PCB does not show optical activity, due to equilibrium
233 between right-hand (*P*) and left-hand (*M*) conformers. BSA addition induced a negative peak at
234 376 nm, while a positive peak appeared at 630 nm in the near-UV/VIS CD spectra (**Fig. 3D**).
235 This pattern is called the positive Cotton effect. Similar to UV/VIS spectra, a new (negative)
236 peak (the "shoulder") was observable at 405 nm. In PCB/BSA samples with molar ratio of 2:1
237 the Cotton effect is markedly higher than in equimolar mixture. In contrast, in samples with 3:1
238 PCB/BSA molar ratio the observed Cotton effect was only negligible higher in comparison with
239 that of 2:1, confirming two specific, high-affinity binding sites for PCB on BSA (**Fig. 3D**).
240 Increasing the PCB concentration in the mixture decreases the ratio between ellipticities at 376
241 and 405 nm, suggesting that the two binding sites have different chirooptical properties.

242 *3.1.4. Molecular docking reveals the position of binding sites for PCB on BSA*

243 We conducted a molecular docking study to determine the BSA binding sites for PCB
244 (**Fig. 4A**). We identified two high-affinity binding sites (**Fig. 4B**), expanding the obtained

245 experimental results. The first binding site for PCB (binding score = –9.7 kcal/mol) was
246 identified between protein domains I and III, named the inter-domain cleft (**Figs. 4C** and **S2A**).
247 Several polar and charged amino acid residues (Thr-183, Glu-186, Arg-427, Arg-435) are
248 involved in the formation of salt bridges/hydrogen bonds with the propionic, pyrrole, and lactam
249 groups of PCB, while residue Tyr-451 is involved in π-π stacking interaction. Residues involved
250 in anion/cation-π electrostatic interactions (Arg-435 and Glu-186) may provide additional
251 stabilization of the PCB-BSA complex (**Figs. 4C** and **S3A**). The second PCB binding site is
252 located at the protein IB subdomain (**Figs. 4D** and **S2B**), with a binding score of –9.6 kcal/mol.
253 Three hydrogen bond/salt bridge interactions exist between the backbone of Leu-115 and the
254 lactam ring, Lys-136 and the lactam ring, and Tyr-160 and the propionic group of PCB (**Figs. 4D**
255 and **S3B**).

### 256 *3.2. Effects of BSA-PCB complex formation*

#### 257 *3.2.1. PCB binding increases the thermal stability of BSA*

258 The decrease in BSA ellipticity at 222 nm following heating, as a consequence of α-
259 helical loss, is useful for studying protein stability. Representative melting curves of BSA in the
260 presence and absence of PCB are shown on **Fig. 5A**. Although the shape of the free protein curve
261 is similar to that of BSA-PCB complexes, it can be seen that PCB inhibits BSA unfolding,
262 especially above 60°C. Indeed, the obtained $T_m$ values suggest thermal stabilization of BSA by
263 PCB binding: the $T_m$ value for free BSA was 73.7°C, the $T_m$ for the BSA-PCB 1:1 molar
264 complex was 75.7°C, and the $T_m$ for the BSA-PCB 1:2 molar complex was the highest, 76.2°C.

### *3.2.2. PCB binding protects BSA from free radical-induced oxidation*

Oxidative modification of BSA was monitored by measuring protein intrinsic fluorescence over time. Fluorescence of BSA exponentially decreases upon addition of AAPH, a generator of free (peroxyl) radicals. In the presence of PCB or Trolox the protein fluorescence decay is slower, and an initial lag phase is detectable (**Fig. 5B**), suggesting a protective effect against protein oxidation. Interestingly, PCB showed higher protective effect than Trolox at the same concentration (**Fig. 5B**). In the presence of 1 μM BSA, the calculated protective effect of 1 μM PCB was 79.4 a.u., whereas that of 2 μM PCB was 4.2-fold higher (330.8 a.u.)~~, suggesting non-linear concentration-activity dependence~~.

### *3.2.3. BSA protects bound PCB from free radical-induced oxidation*

To evaluate the protection against PCB oxidation conferred by complexation with BSA, we tested AAPH-induced PCB oxidation without or with BSA at molar ratios of (protein/pigment) 0.5:1, 1:1, and 5:1. During oxidation, free PCB shows a gradual decrease in absorbance maxima at 620 nm and 360 nm, with simultaneous appearance and increase of two new peaks, at 560 nm and 330 nm. As the concentration of oxidant becomes higher, absorption at 560 nm and 330 nm starts to decrease, and with the further oxidation it is nearly abolished, and PCB becomes completely bleached (**Bhat & Madyastha, 2001**). As can be seen in **Fig. 6A**, without AAPH addition PCB maximum at 620 nm is lower due to formation of PCB-BSA complex, in accordance to **Fig. 3B**. However, 10 min after addition of AAPH, maximum of the BSA-PCB complex at 560 nm was higher than the maximum at 620 nm in non-oxidized complex. In contrast, maximum of 10 min oxidized free PCB at 560 nm is of similar intensity as

286 maximum at 620 nm in non-oxidized free pigment. After 30 min of oxidation (**Fig. 6B**), the 560
287 nm maximum of the oxidized free PCB is decreased, while it is almost preserved in the BSA-
288 PCB complex. The slower decrease of 560 nm maximum in BSA-PCB samples, in comparison
289 to free PCB, suggests that BSA protects bound PCB from further oxidation.

290 To gain further insight into the protective effect of BSA we monitored the percentage of
291 initial absorbance at 620 nm after AAPH addition (**Fig. 6C**). The presence of BSA slowed the
292 decrease in the initial absorbance at 620 nm, suggesting that BSA presence delays PCB
293 oxidation. **Fig. 6D** clearly shows that in free PCB, after AAPH addition, a peak at 560 nm
294 appears, reaches its maximal intensity after 500 s, and then decreases as oxidation proceeds, until
295 it becomes bleached. The presence of BSA delays the start of PCB bleaching to 750 s when
296 bound at a ratio of 0.5:1, and to 950 s at a ratio of 1:1. These results suggest that BSA and PCB
297 protect each other from free radical attack.

298 ***3.2.4. BSA-PCB complex formation masks antioxidant activities of PCB and BSA***

299 The reducing power assay evaluates the ability of antioxidants to reduce potassium
300 hexacyanoferrate(III) to $Fe^{2+}$ ions, and the resulting increase in the absorbance of the reaction
301 mixture is directly proportional to the reducing power of the compound. BSA exhibited much
302 lower reducing power than the equivalent concentration of PCB, whereas BSA-PCB complexes
303 showed lower reducing power than the sum of the free PCB and free BSA (**Fig. 6E**), indicating
304 that PCB binding masked the antioxidant capacity. The calculated masking effect of the reducing
305 power of BSA-PCB complexes with molar ratios 1:1 and 1:2 was similar, at 19% and 18%,
306 respectively.

307 PCB shows high activity in the ORAC assay (**Minic, et. al., 2016**), which measures the
308 capacity of antioxidants to delay peroxyl radical-induced fluorescein degradation. In contrast to
309 the reducing power test, we found that BSA showed higher ORAC values than PCB. Similar to
310 the reducing power test, the sum of the free BSA and free PCB activities was found to be higher
311 than the activity of the corresponding BSA-PCB complex (**Fig. 6F**). The masking effect of the
312 ORAC values of BSA-PCB complexes was 17% and 13%, for molar ratios of 1:1 and 1:2,
313 respectively.

## 314 Discussion

315 We have shown that the highly bioactive food-derived pigment PCB stereo-selectively
316 binds to BSA with high affinity at a molar stoichiometry of 2:1. PCB binding increased the
317 stability of BSA against thermal denaturation and oxidative damage. Complex formation partly
318 masked the antioxidant potential of PCB and BSA. In addition, BSA protects bound PCB from
319 oxidative degradation.

320 Significant quenching of the intrinsic fluorescence of BSA by increasing the amount of
321 PCB indicates strong binding interactions between protein and pigment. Indeed, the measured
322 binding constant ($2.3 \times 10^{6}$ $M^{-1}$) corresponds to that obtained for the HSA-PCB system ($2.2 \times$
323 $10^{6}$ $M^{-1}$) (**Minic, et al., 2015**). The binding affinity of bilirubin ($5 \times 10^{6}$ $M^{-1}$) for BSA is also
324 comparable (**Chen, Song, He, & Yan, 2007**). Further evidence of the binding affinity was
325 obtained from MST experiments. The calculated association constant was slightly lower ($1.4 \times$
326 $10^{6}$ $M^{-1}$), probably because labeling of Lys residues during preparation of BSA samples for MST
327 analysis influenced PCB binding. Synchronous spectra of BSA-PCB complexes did not reveal

328 shifts in the emission maxima of Trp and Tyr residues to indicate their altered microenvironment
329 upon ligand binding. The same pattern was reported for binding of biliverdin to BSA (**Wei, Li,**
330 **Dong, Shuang, Liu, & Huie, 2006**). Strong static quenching of the intrinsic fluorescence of
331 BSA, combined with a much greater contribution of Trp residues in this process, indicates PCB
332 binding near Trp residues of the protein. BSA contains two tryptophan residues: Trp-212 in a
333 hydrophobic binding pocket and Trp-134 on the surface of the molecule (**Bujacz, 2012**). Our
334 docking study has revealed a high-affinity binding site for PCB on the BSA molecule at
335 subdomain IB in close proximity to the Trp-134 residue, but not in subdomain IIA where Trp-
336 212 is located. Indeed, it appears that binding site at subdomain IIA of BSA is more suitable for
337 binding polyphenolic ligands (**Skrt, Benedik, Podlipnik, & Poklar Urlih, 2012**).

338 Rotation around the exocyclic single bond of methine bridges allows PCB to assume
339 various conformations. The cyclic *SSS* conformation is the most stable, with right-hand (*P*) and
340 left-hand (*M*) conformers in equilibrium (**Goller, Strehlow, & Hermann, 2001)**. Binding of
341 PCB to BSA induces optical activity of the pigment, and a positive Cotton effect was observed in
342 the CD spectra of the complexes, suggesting that the *P* conformer is bound to the protein. In
343 contrast, using a similar approach in a previous study, we found that PCB binds to HSA as the *M*
344 conformer (**Minic, et al., 2015**). These differences are not surprising, as previously reported data
345 showed that bilirubin binds to HSA as the *P* conformer, but to BSA as the *M* conformer
346 (**Goncharova, Orlov, & Urbanova, 2013**). Therefore, BSA and HSA have different chiroptical
347 binding properties. Comparison of the near-UV/VIS CD spectra of BSA-PCB complexes at
348 various PCB concentrations showed that saturation of induced ellipticity is reached after addition

349 of two moles of ligand per mole of protein, indicating two sites for binding of PCB to BSA.
350 Subtle differences in the shape of the CD spectra of BSA-PCB between samples, with one or two
351 moles of PCB per mole of BSA, suggested non-equivalence of these two binding sites.

352 Addition of BSA to the PCB solutions caused a visible color change, supporting BSA-
353 PCB complex formation. Changes in the PCB spectra may have been induced by changes in
354 chromophore conformation, protonation state, or polarity **(Dietzek, Maksimenka, Hermann,**
355 **Kiefer, Popp, & Schmitt, 2004; Homoelle & Beck, 1997; Radibratovic, at al., 2016**). Binding
356 of PCB to HSA is followed by a blue shift of the visible spectral band, indicating that bound
357 PCB has a more extended conformation than the free form (**Radibratovic, at al., 2016)**. Red
358 shifts of both the UV and VIS maxima of PCB upon BSA addition implied protonation of the
359 basic nitrogen atom of ring B (**Dietzek, et al., 2004**) probably as a consequence of shifting of the
360 p$K_a$ of pyrrole nitrogen to a higher value, due to protein binding. The US Food and Drug
361 Administration (FDA) has recently approved C-PC from *Spirulina* as a blue food colorant. As
362 PCB is already in use in some parts of the world as a natural food dye (**Mortensen, 2006**), our
363 results predict that addition of both pigment and BSA (protein in general) to food will alter its
364 color in comparison to protein-free products.

365 The results of spectrophotometric titration confirmed binding of approximately two moles
366 of PCB per mole of BSA. The computational (docking) analysis revealed two high-affinity sites
367 on BSA for binding of the mono-anionic form of PCB, one at the inter-domain cleft and the
368 second at the subdomain IB. HSA also binds two PCB molecules, but instead of the inter-domain
369 cleft between domains I and III, one of the binding sites is the cavity of subdomain IIA (**Minic,**

370 **et al., 2015**). This discrepancy is not surprising. Quantitative estimation of changes in the
371 induced CD showed differences between the binding of natural polyphenol (-)-epigallocatechin
372 gallate to BSA and HSA **(Nozaki, Hori, Kimura, Ito, & Hatano, 2009**). Subtle differences
373 between the tertiary structures of the two albumins are the most likely explanation for the partial
374 divergence in the binding location of the tetrapyrrole ligand. Indeed, in the crystal structures of
375 HSA (PDB ID: 1BM0, 4K2C, 4LB9, 5IJF, 3JRY) the distance between the Lys-519 (domain III)
376 and Asp-187 (domain I) residues is too small (0.49–1.28 nm) to accommodate PCB in the inter-
377 domain cleft, as the Lys-519 residue is oriented toward the cleft (**Fig. S4A**). The corresponding
378 distance in the BSA molecule (PDB ID: 3V03, 4JK4, 4F5S, 4OR0) between Lys-520 (domain
379 III) and Glu-186 (domain I) is several times larger (1.92–2.40 nm), with Lys-520 oriented in the
380 opposite direction, therefore allowing PCB to bind deep in this cleft (**Fig. S4B**). The PCB
381 binding site at subdomain IB is highly similar to the binding site of 1-hydroxypyrene, a typical
382 polycyclic hydrocarbon metabolite with four aromatic rings **(Zhang, Chen, Tang, Zhang,**
383 **Chen, Duan, et al., 2016**), and the binding site at the inter-domain cleft is similar to the binding
384 site of Sudan IV, an azo dye that also contains four aromatic rings (**Lu, Zhao, Zhao, Zhang,**
385 **Zhang, Geng, et al., 2011**).

386 Serum albumins are very stable proteins under physiological conditions. Our CD melting
387 curve data showed that the thermal stability of BSA increases following PCB binding. Previous
388 studies have found that food-derived ligands such as fatty acids (**Gumpen, Hegg, & Martens,**
389 **1979**) or saponins **(Ikedo, Shimoyamada, & Watanabe, 1996**) could unambiguously induce
390 thermal stabilization of BSA. PCB binding probably stabilized BSA by decreasing protein

391 flexibility, similar to its thermal stabilization of HSA **(Radibratovic, at al., 2016**). Indeed, it was
392 found that BSA thermal stabilization induced by ligand binding correlates with changes in
393 protein flexibility (**Celej, et al., 2003**).
394 Oxidative modifications of serum albumins are responsible for their altered biological
395 properties, including intrinsic antioxidant and binding properties (**Oettl & Stauber, 2007**). The
396 strong antioxidant capacity of PCB was demonstrated in various model systems **(Hirata,**
397 **Tanaka, Ooike, Tsunomura, & Sakaguchi, 2000; Minic, et al., 2016**). Our results indicate that
398 efficient PCB binding inhibits peroxyl radical-induced BSA oxidation, confirming the ability of
399 the chromophore to protect proteins from oxidative stress. The protective effect was estimated to
400 be 4.2-fold higher with saturated binding then when only half of the BSA binding sites were
401 occupied with PCB. The distance between the exposed Trp-134 and PCB is much shorter when
402 ligand is bound at the IB subdomain than at the inter-domain cleft (0.63 nm *vs.* 2.13 nm,
403 respectively). ~~At a BSA/PCB molar ratio of 1:2, the second binding site is occupied and binding~~
404 ~~of PCB near Trp increases its ability to protect this residue from oxidation, compared to when~~
405 ~~only the first binding site is occupied.~~ Taken together, these data indicate that PCB preferentially
406 binds to the site in the cleft, protecting Trp residues, but when it saturates the IB site as well,
407 closer to Trp, it provides more effective protection. ~~This suggests that bound PCB could not only~~
408 ~~prevent protein oxidation, but also protect albumin-bound fatty acids from free radical oxidation,~~
409 ~~as shown for HSA-bilirubin complexes (**Stocker, Glazer, & Ames, 1987**).~~
410 Interestingly, the antioxidant capacity of PCB in complex with BSA is apparently lower
411 than the sum of antioxidant capacities of the free pigment and free BSA. We found (**Fig. 6**) that

412 the reducing power and ORAC values of BSA-PCB complexes were consistently smaller (up to
413 20%) than the simple sum of the individual BSA and PCB activities. It is well known that
414 binding of antioxidants to food proteins, including BSA, can mask their antioxidant capacity
415 (**Arts, Haenen, Voss, & Bast, 2001; Stojadinovic, et al., 2013**) and consequently their *in vivo*
416 activities (**Serafini, Ghiselli, & Ferro-Luzzi, 1996**). However, the masking effect should not be
417 regarded as a decrease in the antioxidant potential of both complex actors, as proteolysis of BSA
418 during digestion would release free PCB, with full antioxidant potential. The antioxidant activity
419 of free antioxidant, such as quercetin, decreases over time due to degradation, whereas nano-
420 encapsulation of antioxidant into BSA reduced its initial antioxidant activity, due to the masking
421 effect of the protein matrix. However, over time the antioxidant activity of the trapped
422 antioxidants increases due to its protection (**Antonio, Khalil, & Mainardes, 2016**).

423 We further demonstrated that the protective effect against free radical-induced oxidation
424 is mutual, e.g. that BSA also protects PCB. Therefore, the results of this study relate to
425 protection of PCB used as a food coloring, and especially as a bioactive component. It has been
426 shown that BSA can substantially protect bound bilirubin from hydroxyl radical attack
427 (**Adhikari & Gopinathan, 1996**). The binding of β-carotene to BSA efficiently protects the
428 ligand against photo-oxidation, because the excitation energy is dissipated into the protein matrix
429 rather than driving the photochemical reaction (**Chang, Cheng, Han, Zhang, & Skibsted,
430 2016**). As PCB is a highly conjugated system, similar to carotenoids and therefore
431 photosensitive, BSA is also expected to protect bound PCB from photooxidation. The mutually
432 protective effect of complexed PCB and BSA against free radical attack, by delay of oxidative

433 degradation, can be explained by the fact that interacting redox-active species, such as PCB and
434 reactive amino acid resides in the protein, can transfer electrons and/or hydrogen atoms to each
435 other, promoting mutual regeneration.

## 436 Conclusions

437 In this paper, we examined the binding of bioactive PCB from the dietary supplement
438 Spirulina to BSA, using multiple spectroscopic methods and a molecular docking technique.
439 Based on the results of the protein fluorescence quenching study and microscale thermophoresis,
440 high-affinity binding of PCB to BSA was confirmed. Spectrophotometric titration data,
441 supported by a computational (molecular docking) approach, revealed two PCB binding sites on
442 BSA, and CD spectroscopy indicated that the *P* conformer of the pigment binds to the protein.
443 Contrary to HSA, BSA has the ability to accommodate PCB into the inter-domain cleft, together
444 with the IB subdomain. In the second part of this study, the effects of binding on selected protein
445 and ligand features were examined. BSA in complex with PCB was more resistant to thermal
446 denaturation than free protein, and complex formation partly masked the antioxidant properties
447 of bound PCB and BSA. However, when in complex, the ligand and protein showed mutually
448 protective effects against free radical-induced oxidation, reflected in delay of oxidative
449 degradation of both species. In addition, our results indicated subtle differences between binding
450 of PCB with bovine *vs.* human serum albumin.

451 Delivery and protection of sensitive redox-active health-promoting compounds is an
452 important challenge. Although many biodegradable materials have been developed, BSA is
453 widely used in drug delivery systems due to its easy purification, abundance, low cost, excellent

454 binding properties, and its wide acceptance in the food and pharmaceutical industries. Similar to
455 other sensitive bioactive ligands, such as polyphenols (**Kumar, Meena, & Rajamani, 2016**),
456 PCB shows potential for encapsulation into BSA-based nanoparticles, to improve PCB stability
457 and protect its activity during prolonged storage. In addition, due to the demonstrated high-
458 affinity binding of PCB to BSA, PCB encapsulated into a BSA matrix could be used as a
459 functional food additive that provides color and as well as bioactivity.

460 **Note:** The authors declare no conflict of interest.

461 **Acknowledgments**

462 The authors are grateful to Dr. Marek Zurawski (NanoTemper Technologies GmbH,
463 Germany) for assistance in obtaining and processing MST data. The Ministry of Education,
464 Science and Technological Development of the Republic of Serbia (Grant Number 172024) and
465 FP7 RegPot project FCUB ERA GA No. 256716 supported this work. The EC does not share
466 responsibility for the content of the article.

467 **References**

468 Adhikari, S., & Gopinathan, C. (1996). Oxidation reactions of a bovine serum albumin-bilirubin
469 complex. A pulse radiolysis study. *International Journal of Radiation Biology, 69*(1), 89-
470 98.

471 Antonio, E., Khalil, N. M., & Mainardes, R. M. (2016). Bovine Serum Albumin Nanoparticles
472 Containing Quercetin: Characterization and Antioxidant Activity. *Journal of Nanoscience*
473 *and Nanotechnology, 16*(2), 1346-1353.

474 Arts, M. J., Haenen, G. R., Voss, H. P., & Bast, A. (2001). Masking of antioxidant capacity by
475 the interaction of flavonoids with protein. *Food and Chemical Toxicology, 39*(8), 787-791.
476 Bhat, V. B., & Madyastha, K. M. (2001). Scavenging of peroxynitrite by phycocyanin and
477 phycocyanobilin from Spirulina platensis: protection against oxidative damage to DNA.
478 *Biochemical and Biophysical Research Communications, 285*(2), 262-266.
479 Bujacz, A. (2012). Structures of bovine, equine and leporine serum albumin. *Acta*
480 *Crystallographica Section D Biological Crystallography, 68*(Pt 10), 1278-1289.
481 Buono, S., Langellotti, A. L., Martello, A., Rinna, F., & Fogliano, V. (2014). Functional
482 ingredients from microalgae. *Food & Function, 5*(8), 1669-1685.
483 Celej, M. S., Montich, G. G., & Fidelio, G. D. (2003). Protein stability induced by ligand binding
484 correlates with changes in protein flexibility. *Protein Science, 12*(7), 1496-1506.
485 Chang, H. T., Cheng, H., Han, R. M., Zhang, J. P., & Skibsted, L. H. (2016). Binding to Bovine
486 Serum Albumin Protects beta-Carotene against Oxidative Degradation. *Journal of*
487 *Agricultural and Food Chemistry, 64*(29), 5951-5957.
488 Chen, J., Song, G., He, Y., & Yan, Q. (2007). Spectroscopic analysis of the interaction between
489 bilirubin and bovine serum albumin. *Microchimica Acta, 159*(1-2), 79-85.
490 Dietzek, B., Maksimenka, R., Hermann, G., Kiefer, W., Popp, J., & Schmitt, M. (2004). The
491 excited-state dynamics of phycocyanobilin in dependence on the excitation wavelength.
492 *Chemphyschem, 5*(8), 1171-1177.
493 Eriksen, N. T. (2008). Production of phycocyanin--a pigment with applications in biology,
494 biotechnology, foods and medicine. *Applied Microbiology and Biotechnology, 80*(1), 1-14.

495 Fernández-Rojas, B., Hernández-Juárez, J., & Pedraza-Chaverri, J. (2014). Nutraceutical
496 properties of phycocyanin. *Journal of Functioanl Foods, 11*, 375-392.
497 Fuentes Aparicio, V., Sanchez Marcen, I., Perez Montero, A., Baeza, M. L., & de Barrio
498 Fernandez, M. (2005). Allergy to mammal's meat in adult life: immunologic and follow-up
499 study. *Journal of Investigational Allergology and Clinical Immunology, 15*(3), 228-231.
500 Goller, A. H., Strehlow, D., & Hermann, G. (2001). Conformational flexibility of
501 phycocyanobilin: An AM1 semiempirical study. *Chemphyschem, 2*(11), 665-671.
502 Goncharova, I., Orlov, S., & Urbanova, M. (2013). The location of the high- and low-affinity
503 bilirubin-binding sites on serum albumin: ligand-competition analysis investigated by
504 circular dichroism. *Biophysical Chemistry, 180-181*, 55-65.
505 Gumpen, S., Hegg, P. O., & Martens, H. (1979). Thermal stability of fatty acid-serum albumin
506 complexes studied by differential scanning calorimetry. *Biochimica et Biophysica Acta,*
507 *574*(2), 189-196.
508 Hirata, T., Tanaka, M., Ooike, M., Tsunomura, T., & Sakaguchi, M. (2000). Antioxidant
509 activities of phycocyanobilin prepared from Spirulina platensis. *Journal of Applied*
510 *Phycology, 12*, 435–439.
511 Homoelle, B. J., & Beck, W. F. (1997). Solvent accessibility of the phycocyanobilin
512 chromophore in the alpha subunit of C-phycocyanin: implications for a molecular
513 mechanism for inertial protein-matrix solvation dynamics. *Biochemistry, 36*(42), 12970-
514 12975.
515 Ikedo, S., Shimoyamada, M., & Watanabe, K. (1996). Interaction between Bovine Serum

516 Albumin and Saponin As Studied by Heat Stability and Protease Digestion. *Journal of*
517 *Agricultural and Food Chemistry, 44*, 792-795.
518 Jakobek, L. (2015). Interactions of polyphenols with carbohydrates, lipids and proteins. *Food*
519 *Chemistry, 175*, 556-567.
520 Kumar, S., Meena, R., & Rajamani, P. (2016). Fabrication of BSA-Green Tea Polyphenols-
521 Chitosan Nanoparticles and Their Role in Radioprotection: A Molecular and Biochemical
522 Approach. *Journal of Agricultural and Food Chemistry, 64*(30), 6024-6034.
523 Livney, Y. D. (2010). Milk proteins as vehicles for bioactives. *Current Opinion in Colloid &*
524 *Interface Science, 15*(1-2), 73-83.
525 Lu, D., Zhao, X., Zhao, Y., Zhang, B., Zhang, B., Geng, M., & Liu, R. (2011). Binding of Sudan
526 II and Sudan IV to bovine serum albumin: comparison studies. *Food and Chemical*
527 *Toxicology, 49*(12), 3158-3164.
528 McCarty, M. F. (2007). Clinical potential of Spirulina as a source of phycocyanobilin. *Journal of*
529 *Medicinal Food, 10*(4), 566-570.
530 Minic, S. L., Milcic, M., Stanic-Vucinic, D., Radibratovic, M., Sotiroudis, T. G., Nikolic, M. R.,
531 & Velickovic, T. Ć. (2015). Phycocyanobilin, a bioactive tetrapyrrolic compound of blue-
532 green alga Spirulina, binds with high affinity and competes with bilirubin for binding on
533 human serum albumin. *RSC Advances, 5*(76), 61787-61798.
534 Minic, S. L., Stanic-Vucinic, D., Mihailovic, J., Krstic, M., Nikolic, M. R., & Cirkovic
535 Velickovic, T. (2016). Digestion by pepsin releases biologically active chromopeptides
536 from C-phycocyanin, a blue-colored biliprotein of microalga Spirulina. *Journal of*

537 *Proteomics, 147*, 132-139.

538 Mortensen, A. (2006). Carotenoids and other pigments as natural colorants. *Pure and Applied*
539 *Chemistry, 78*(8).

540 Nozaki, A., Hori, M., Kimura, T., Ito, H., & Hatano, T. (2009). Interaction of polyphenols with
541 proteins: binding of (-)-epigallocatechin gallate to serum albumin, estimated by induced
542 circular dichroism. *Chemical and Pharmaceutical Bulletin (Tokyo), 57*(2), 224-228.

543 Oettl, K., & Stauber, R. E. (2007). Physiological and pathological changes in the redox state of
544 human serum albumin critically influence its binding properties. *British Journal of*
545 *Pharmacology, 151*(5), 580-590.

546 Ofori, J. A., & Hsieh, Y.-H. P. (2012). The Use of Blood and Derived Products as Food
547 Additives. In Y. El-Samragy (Ed.), *Food Additive*. Rijeka, Croatia: InTech.

548 Ou, B., Hampsch-Woodill, M., & Prior, R. L. (2001). Development and validation of an
549 improved oxygen radical absorbance capacity assay using fluorescein as the fluorescent
550 probe. *Journal of Agricultural and Food Chemistry, 49*(10), 4619-4626.

551 Oyaizu, M. (1986). Studies on product of browningreaction prepared form glucosamine.
552 *Japanese Journal of Nutrition, 44*, 307-315.

553 Peters, T. J., (1995). *All About Albumin Biochemistry, Genetics, and Medical Applications*:
554 Academic Press.

555 Radibratovic, M., Minic, S., Stanic-Vucinic, D., Nikolic, M., Milcic, M., & Cirkovic Velickovic,
556 T. (2016). Stabilization of Human Serum Albumin by the Binding of Phycocyanobilin, a
557 Bioactive Chromophore of Blue-Green Alga Spirulina: Molecular Dynamics and

558 Experimental Study. *PLoS One, 11*(12), e0167973.
559 Serafini, M., Ghiselli, A., & Ferro-Luzzi, A. (1996). In vivo antioxidant effect of green and black
560 tea in man. *European Journal of Clinical Nutrition, 50*(1), 28-32.
561 Skrt, M., Benedik, E., Podlipnik, Č., & Poklar Urlih, N. (2012). Interactions of different
562 polyphenols with bovine serum albumin using fluorescence quenching and molecular
563 docking. *Food Chemistry*, 135(4), 2418-2424.
564 ~~Stocker, R., Glazer, A. N., & Ames, B. N. (1987). Antioxidant activity of albumin-bound~~
565 ~~bilirubin. *Proceedings of the National Academy of Sciences of the United States of*~~
566 ~~*America, 84*(16), 5918-5922.~~
567 Stojadinovic, M., Radosavljevic, J., Ognjenovic, J., Vesic, J., Prodic, I., Stanic-Vucinic, D., &
568 Cirkovic Velickovic, T. (2013). Binding affinity between dietary polyphenols and beta-
569 lactoglobulin negatively correlates with the protein susceptibility to digestion and total
570 antioxidant activity of complexes formed. *Food Chemistry, 136*(3-4), 1263-1271.
571 Trott, O., & Olson, A. J. (2010). AutoDock Vina: improving the speed and accuracy of docking
572 with a new scoring function, efficient optimization, and multithreading. *J Comput Chem,*
573 *31*(2), 455-461.
574 Wei, Y. L., Li, J. Q., Dong, C., Shuang, S. M., Liu, D. S., & Huie, C. W. (2006). Investigation of
575 the association behaviors between biliverdin and bovine serum albumin by fluorescence
576 spectroscopy. *Talanta, 70*(2), 377-382.
577 Wienken, C. J., Baaske, P., Rothbauer, U., Braun, D., & Duhr, S. (2010). Protein-binding assays
578 in biological liquids using microscale thermophoresis. *Nature Communications, 1*, 100.

Zhang, J., Chen, W., Tang, B., Zhang, W., Chen, L., Duan, Y., Zhu, Y., Zhud, Y., & Zhang, Y. (2016). Interactions of 1-hydroxypyrene with bovine serum albumin: insights from multi-spectroscopy, docking and molecular dynamics simulation methods. *RSC Advances, 6*, 23622-23633.

## Figure captions

**Figure 1. BSA fluorescence quenching by PCB. (A)** Emission spectra (excitation at 280 nm) of BSA (0.25 μM) in the presence of different concentrations of PCB (0, 0.05, 0.1, 0.15, 0.2, 0.25, 0.3, 0.35, 0.4, 0.5, 0.6, 0.7, and 0.8 μM, for curves a to m, respectively). Dot line represents 0.8 μM PCB; (**B**) Stern-Volmer plots of BSA fluorescence quenched by PCB. Error bars represent the standard deviation (n = 3); Synchronous fluorescence spectra of BSA (0.25 μM) with (**C**) $\Delta\lambda = 60$ nm (Trp) and with (**D**) $\Delta\lambda = 15$ nm (Tyr) in the presence of increasing concentrations of PCB (0–0.8 μM) for curves a to m, respectively.

**Figure 2. BSA-PCB microscale thermophoresis (MST). (A)** MST time traces of fluorescently labeled BSA (1.5 μM) in the presence of different concentrations of PCB (from 3 to $10^5$ nM, for curves a to p, respectively); (**B**) MST binding curve for PCB interaction with BSA. Error bars represent the standard deviation (n = 3).

**Figure 3. Monitoring of BSA-PCB binding. (A)** Color change of concentrated PCB solution upon addition of BSA (150 μM each); (**B**) Effect of BSA addition (0, 10, 20, and 40 μM, for curves a to d, respectively) on the UV/VIS absorption spectra of 20 μM PCB. Dot line represents 40 μM BSA; **(C)** Determination of binding stoichiometry for BSA-PCB complex by monitoring

599 decreasing PCB absorbance at 365 nm. Points colored in black and blue were used for
600 extrapolation to determine the intersection point. Error bars represent the standard deviation (n =
601 3); (**D**) Effect of PCB addition (10, 20, and 30 μM, for curves a to c, respectively) on the near
602 UV/VIS CD spectra of 10 μM BSA. The dotted line represents 10 μM PCB in the absence of
603 BSA.

604 **Figure 4. Docking of the BSA-PCB complex. (A)** Chemical structure of PCB; **(B)** The ribbon
605 model of the BSA protein (PDB ID: 3v03) with labeled subdomains. Bound PCB and Trp
606 residues are shown in purple and red in the space-filling representation, respectively; 2D diagram
607 with labeled interactions of docked PCB to BSA (PDB ID: 3V03) at two proposed binding sites:
608 Inter-domain cleft **(C)** and subdomain IB **(D)**.

609 **Figure 5. Effects of BSA-PCB binding on protein stability. (A)** Curves for temperature
610 dependence of 0.5 μM BSA ellipticity at 222 nm in the absence and presence of 0.5 and 1 μM
611 PCB; **(B)** BSA (1 μM) fluorescence decay after addition of the free radical generator AAPH in
612 the absence and presence of PCB (1 or 2 μM) and Trolox (2 μM).

613 **Figure 6. Effects of BSA-PCB binding on ligand stability and antioxidant activity of PCB**
614 **and BSA.** UV/VIS spectra of PCB with/without BSA after 10 min **(A)** and after 30 min **(B)** upon
615 AAPH addition (dash lines). The samples without AAPH are shown as solid lines on both
616 graphs; Monitoring of PCB oxidative degradation by AAPH, with and without BSA, as a
617 percentage of the initial absorbance at 620 nm after AAPH addition **(C)** and formation and
618 disappearance of the peak at 560 nm **(D)**; Reducing power (absorbance) of free BSA, free PCB,
619 and BSA-PCB complexes **(E)**; ORAC values (TE) of free BSA, free PCB, and BSA-PCB

620 complexes (**F**). Error bars represent the standard deviation (n = 3).

621

622 ## Highlights

623 - Phycocyanobilin (PCB) from Spirulina binds to BSA with high affinity at two sites
624 - PCB stereo-selectively binds at the inter-domain cleft and at subdomain IB
625 - PCB binding increases the thermal stability of BSA
626 - PCB and BSA are mutually protective against free radical-induced oxidation
627 - BSA can serve as a suitable delivery system for PCB

628

629